Official publication of Pakistan Phytopathological Society
Pakistan Journal of Phytopathology
ISSN: 1019-763X (Print), 2305-0284 (Online)
http://www.pakps.com

FOURIER-TRANSFORM INFRARED SPECTROSCOPY IDENTIFIED CHANGES IN THE CELL WALL COMPONENTS ASSOCIATED WITH THE SIMULTANEOUS TRAFFICKING OF WHITE MOLD FUNGUS AND COPPER

Amna Shoaib*, Nafisa, Ghanwa Riaz, Qudsia Fatima, Uswa Fatima, Nimra Iqbal

Department of Plant Pathology, Faculty of Agricultural Sciences, University of the Punjab, Lahore, Pakistan.

A B S T R A C T

Fourier-transform infrared spectroscopy (FTIR) was found a fast and efficient tool to identify compositional alterations in the cell wall of *Pisum sativum* L. (green pea) growing in copper [Cu(II)]-spiked and *Sclerotium rolfsii* (SR) inoculated soil. In the current study, the separate and combined effect of *S. rolfsii* and Cu(II) was assessed on cell wall biochemistry and Cu accumulation in the pea plants. Data regarding metal content, bioaccumulation factors, and translocation factors revealed that 90-day-old green pea plants could handle metal stress by restricting Cu(II) translocation from root to shoot. Soil FTIR showed shifting in kaolinite and quartz peaks after binding with Cu(II) and SR. Cu(II) and SR induced major changes in the protein and carbohydrate regions of the plants.

Keywords: Copper, Bioaccumulation factors, Metal accumulation, Sclerotia.

INTRODUCTION

Green peas (*Pisum sativum* L.) or garden peas are the fourth-most extensively cultivated grain legume in the world. Southern blight is a serious and frequent soil-borne fungal disease of field peas caused by *Sclerotium rolfsii* Sacc., is a basidiomycete fungus, responsible for yield losses massively, has evolved an arsenal of tools to penetrate and break down the cell wall, therefore, making it an aggressive pathogen of over 500 plant species (Nafisa *et al*., 2013, 2016). The fungal sclerotia (compact mass of hardened fungal mycelium) can stay in the soil for 5-10 years even under extreme conditions, making it a difficult pathogen to get rid (Sana *et al.,* 2016; Nafisa *et al*., 2016; Rafi *et al*., 2017). Cu-based fungicides have been frequently utilized against such devastating plant diseases. Metal in fungicides has led to a detrimental influence on plant primary production and even survival through the remodeling of the cell wall (Shoaib *et al*., 2022). Although Cu is an essential player in electron transport, but the range of 5-30 mg/kg dry weight is considered as the physiological amount of Cu in plants (Printz *et al*., 2016). It has been predicted that Cu in soil may reach at a toxic level, i.e., 3000 mg/kg on account of 2 to 4 kg Cu/ha/year application of Cu-based fungicide (Alloway, 2013). The ability of *S. rolfsii* to tolerate a wide range of chromium concentrations (100-300 ppm) through evolving defense mechanisms has been reported (Sana *et al*., 2017; Rafi *et al*., 2017). Plants have evolved multi-layered defense systems in the form of cell wall that expands their function as passive defensive barriers to cope with adverse exogenous stimuli (Khurshid et *al.*, 2017; Akhtar and Shoaib, 2020; Shoaib *et al*., 2021, 2022). Changes in the biochemical composition of the cell wall reflect the overall changes in the metabolic processes, and these changes can be addressed adequately using Fourier transform infrared (FTIR) spectroscopy (Shoaib *et al*., 2013a; Bağcıoğlu *et al*., 2017).

In contrast with the other methods, FTIR is making substantial headway in the biological sciences as a novel, simple, rapid, and powerful technique (Largo-

Submitted: October 22, 2022
Revised: November 01, 2022
Accepted for Publication: December 05, 2022
* Corresponding Author:
Email: amna.iags@pu.edu.pk

Gosens *et al*., 2014). FTIR provides a snapshot of biochemical composition in plant tissues or cells to analyze spectrum based on the vibrations of bonds within functional groups that can be considered as a biochemical or metabolic "fingerprint" (Bağcıoğlu *et al*., 2017). The configuration of molecular functional assemblies can be achieved based on peak width, position, and the intensity of absorption (Mazurek *et al*., 2013). Each functional group in a molecule has characteristic absorption frequencies in the IR spectrum in the range of 4000 and 400 cm^{-1}, which reveals the absorbance bands uniquely assigned to cellular components involved in plant growth and development. For instance, 1700-1600 cm^{-1} associated with the secondary structure of the protein amide-I consisted of the peptide bond (C=O: 80%; N–H: 20%), and the 1200–1000 cm^{-1} belongs to the carbohydrate fingerprint region (C–O) (Wilson *et al*., 2000). Thumanu *et al*. (2015) findings revealed that variations in absorbance intensities of IR regions of the cell wall at different frequencies can be related to the activation of enzymes in the plant cell walls of the epidermis. Khurshid *et al*. (2017) also related changes in the carbohydrate and protein of cell walls in tomato plants to the stress response incited by *Fusarium oxyspourum* f.sp. *lycopersici* and chromium (Cr). Lahlali *et al*. (2014), identified biochemical changes in the wheat cell wall (i.e. lignin, cellulose, and hemicellulose) infected by *Fusarium graminearum*, and connected to mechanisms of this resistance. Therefore, biochemical interpretation with respect to lipids, carbohydrates, and proteins of plant biomass using FTIR can be used as supportive in biomolecule characterization and unraveling stress adapt mechanisms in plants (Rafi *et al*., 2017; Nikalje *et al*., 2019). The present investigation was conducted to investigate the separate and combined effect of *S. rolfsii* and Cu(II) on biochemical alterations in *P. sativum* cell wall through FTIR technique along with the determination of metal accumulation in the pea plants.

MATERIAL AND METHODS

Experiment: This experiment was an extension of our previous work (Nafisa *et al*., 2016). Cu(II) solution prepared from $CuSO_4.5H_2O$ (MERCK) was spiked in the soil. This metal-spiked soil was left for 10 days for homogenization and air-drying. The metal-spiked soil was then sieved (2 mm mesh size), filled in pots (5 kg in 12 × 10 cm pot), and inoculated with 100 mL of mycelial suspensions of *S. rolfsii* (SR). Green pea var. Meteor seeds were surface sterilized with 0.5% sodium hypochlorite solution and were sown (15 seeds pot^{-1}) in the triplicate set of the treatments, kept under randomized design (25º C ± 3; 12 h photoperiod and 70% relative humidity). **T_1:** control; **T_2:** SR (*S. rolfsii*) inoculated soil; **T_3:** Cu-spiked soil, and **T_4:** Cu-spiked + SR inoculated soil.

Copper analysis, BAF and TF: After 90 days of sowing, the measured amount of dried samples of roots, shoots, and pods from each treatment was digested with nitric acid and was analyzed for Cu concentration through a Z-5000 Polarized Zeeman Atomic absorption spectrophotometer. Bioaccumulation factors (BAF) and translocation factor (TF) in plant parts were calculated by using the following formulae (Yashim *et al.,* 2014).

$$\text{BAF} = \frac{\text{Concentration of metal in plant}}{\text{Concentration of metal in soil}}$$

$$\text{TF} = \frac{\text{Metal conc. in above ground tissues}}{\text{Metal conc. in root}}$$

FTIR analysis: MIDAC M series 2003 was employed for IR spectra of the soil, roots, and shoots the following protocol of Khurshid *et al*. (2017). To obtain a diffuse reflectance IR spectrum, a uniform thin pellet was prepared by homogenizing a dried sample (1 mg) with potassium bromide (2.5 mg). The IR spectrum of each sample was observed in the mid-infrared range at room temperature (26 °C).

RESULTS

Metal accumulation by the green pea plant: Plants in T_1 (control) and T_2 (SR) did not contain Cu(II). The plants uptake significantly greater amounts of Cu from the Cu-spiked in T_3, hence the roots, shoots, and pods showed 206, 4.35 and 3.57 mg/kg and in T_4 [(Cu(II) + SR], it was 220, 5.29 and 4.38 mg/kg dry weight of plant, respectively. The BAF (capacity of the plant to uptake heavy metal from the surrounding environment) and TAF (translation from root to above-ground parts) were less than one (Table 1).

FTIR spectral analysis: Characteristic functional groups contributing to the formation of absorption bands at specific wave numbers are indicated in the Table 2.

IR spectral analysis of soil: FTIR absorption spectra of the soil before and after exposure to either pathogen (T_2) or metal alone (T_3) or in combination (T_4) portrayed intricate additive images of their overall chemical composition and possible

interactions (Table 2 and 3; Figure 1). A total of 10 peaks (3696, 3625, 3600, 1633, 1425, 1030, 785, 695, 520, and 497 cm^{-1}) were observed in raw soil (T_1). Most of the bands such as 3696, 3625, 1030, 785, 695, 520, and 497 cm^{-1} showed the presence of kaolinite [$Al_2Si_2O_5(OH)_4$] and quartz (SiO_2), while peaks at 3625 cm^{-1}, 1610-1623 cm^{-1}, 1030 cm^{-1} represent the occurrence of gypsum and peaks at 695, 520, and 497 cm^{-1} illustrate the represented calcite. All those peaks either disappeared or shifted to low wave numbers after soil inoculation with the pathogen and spiking with the Cu.

Table 1. Heavy metal contents in different parts of 90 days old *Pisum sativum* plant.

Treatments	Heavy metal contents (µg/kg dry weight)			Bioaccumulation factor	Translocation factor
	Roots	Shoots	Pods		
Cu(II)	206±1.2 b	4.35±0.13 b	3.57±0.01 b	0.67±0.02 b	0.046±0.03 b
Cu(II) + SR	220±4.4 a	5.29±0.07 a	4.38±0.03 a	0.87±0.01 a	0.043±0.01 a

Alphabets in each column show the significant differences as determined by the LSD.

Table 2. General band assignment of the mid-IR spectrum.

Frequency (cm^{-1})	Assignments
Mid-IR spectrum of soil	
3670-3656	O–H str.
	O–H (crystalline hydroxyl)
	H-O-H str., absorbed water
1642-1569	O-H, bend water, C-H str.
1035-1030	Si-O str. clay minerals
800-784	OH deformation, linked to Al, and Mg (Si-O quartz)
700-886	Si–O str., Si–O–Al str. (Si-O quartz)
542-535	Si–O str., Si–O–Al str. (Fe-O, Fe_2O_3, Si-O-Al str.)
475-468	Si–O str., Si–O–Fe str. (Si-O-Si bend)
Mid-IR spectrum of plants	
3500-3200	O–H and N–H stretch: carbohydrates, proteins, alcohols, and phenolic compounds
2930-2920	CH_2 asymmetric stretch: Mainly lipids
1650-1630	Amide I (C=O stretch): protein, pectin, water-associated cellulose or lignin, alkaloids
1560-1540	Amide II (C=N and N–H stretch): Mainly protein
1515-1505	C=C aromatic stretch: lignin
1430-1420	O–H bend: cell wall polysaccharide, alcohol, and carboxylic acid
1085-1075	C–O deformation: secondary alcohol, aliphatic ester
1045-1030	O–H and C–OH stretch: cell wall polysaccharides (arabinan, cellulose)

IR spectral analysis of roots and shoot: In the control sample of T_1, the region at 3400-3200 cm^{-1} showed the presence of the O–H or N–H stretching modes of carbohydrates, adsorbed water, and proteins. The band at 2929-2857 cm^{-1} are due to hydrophobic CH_2 asymmetrical and symmetrical stretching vibrations, respectively, while 1638-1430 cm^{-1} reveal the O–H bending, amide I and II (N–C=O) of protein and pectic acid esters, H-bonded C=O of conjugated ketones, and 1084-1059 cm^{-1} indicating C–O and C–C stretching vibrations (Tables 2 and 3; Figure 2).

In comparison to T_1, the soil inoculated with the *S. rolfsii* (T_2) induced changes in the carbohydrates and protein in the root and shoot by exhibiting a reduction in their wave number. Besides, in T_2, new peaks in the root (3427 and 3296 cm^{-1}) and shoot (3421 and 3445 cm^{-1}) regions of the carbohydrates were also present. The lipid region of the roots showed intensified wavenumber of 2931 cm^{-1}, while the shoot exhibited a reduction in the wave number of 2917 cm^{-1} with the absence of symmetrical stretching vibrations relative to T_1 (root: 2929 cm^{-1}, shoot: 2924 and 2857 cm^{-1}). The peak values in the protein region decreased (T_1/T_2, root: 1638/1634; shoot: 1628/1625, 1430/1423 cm^{-1}), while many peak values found in T_1 at 1434 cm^{-1} (root), and 1546 and 1323 cm^{-1} (shoot) were absent in T_2 with the additional peak at 1398 cm^{-1}. The carbohydrates regions were also indicated by a new peak at 1030 cm^{-1} (shoot) and reduction (T_1/T_2, root: 1059/1030 cm^{-1} and shoot: 1084/1083 cm^{-1}) in the band intensity as compared to the control (Tables 2 and 3; Figure 2).

Cu-spiking in soil (T_3) caused the appearance of many additional peaks (root: 3428, 3285, 1539, 1515, and 1083 cm^{-1}; shoot: 3264 and 1635 cm^{-1}) due to the association of Cu with these regions (3500 to 3200 cm^{-1}). Cu also

induced alterations in the peak intensity of carbohydrate (3450 to 3210 cm^{-1}), protein (1643-1420 cm^{-1}), as well as lipid (2930 cm^{-1}) regions of root and shoot along with the disappearance of a few peaks, nonetheless, more changes were observed in root spectra (Table 2 and 3; Figure 2).

In the combined effect of *S. rolfsii* and Cu (T_4), homologous regions of macromolecule altered as was recorded with the individual effect of *S. rolfsii* (T_2) and metal (T_3), though with the more intense changes in the band intensity. For instance, the carbohydrate-associated region exhibited the appearance of three new peaks (3428, 3240, and 3210 cm^{-1}), with a reduction in the peak intensity at 3264 cm^{-1} and the disappearance of other peaks in these regions with regard to T_1. Moreover, any increase or decrease in the intensity of the band in the protein region (1642-1525 cm^{-1}) was more similar to T_3 (Table 2 and 3; Figure 2).

Table 3. Important IR bands of soil, root, and shoot samples.

Control (T_1)	SR (T_2)	Cu(II) (T_3)	SR + Cu(II) (T_4)
SOIL			
3696, 3625, 3600			3619
	3424	3426	3400
1633	1623	1610	1610
1425		1427	1429
1030			1030
785			
695		683	
520			
497		476	470
ROOT			
3383	3365	3355	
	3427, 3296	3428, 3285	3264
2929	2931	2931	2934
1638	1634	1643	1642
		1539, 1515	1525
1434	1398		1427
1059	1030	1083, 1043	1080
SHOOT			
3399, 3364, 3336	3395, 3421, 3445	3426	3428
3287		3285	3264, 3240, 3210
2924, 2857	2917	2923	2929
1628	1625	1635, 1624	1635, 1624
1546			
1430	1423		
1323			1384
1084	1083, 1030	1091, 1046	1036

The peak number highlighted in blue indicates the change in wave number as compared to the control.
The peak number highlighted in green indicates additional peaks as compared to the control.

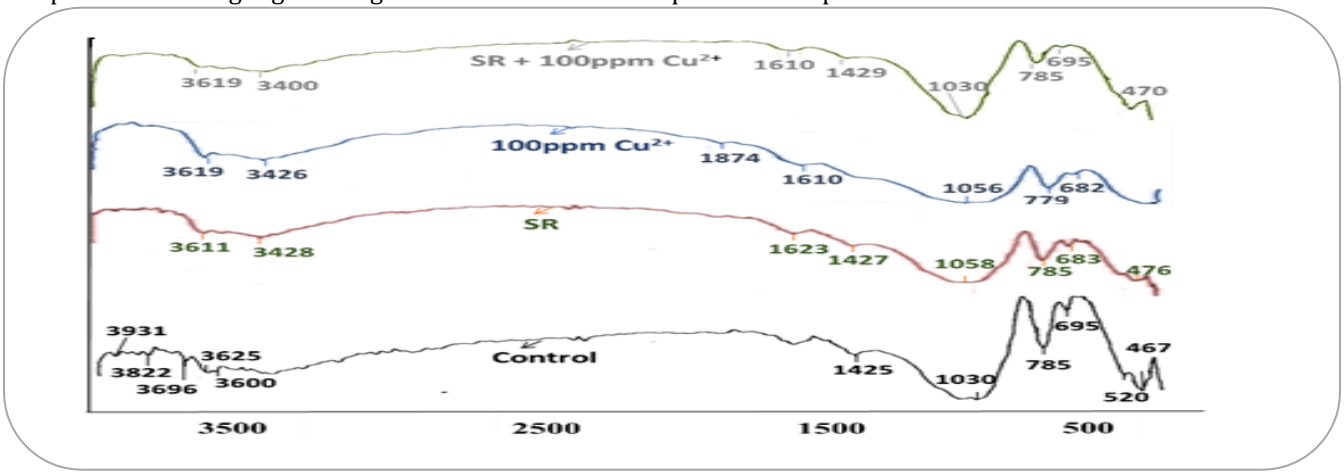

Figure 1. Comparison and characterization of Infrared spectra of soil around *Pisum sativum*.

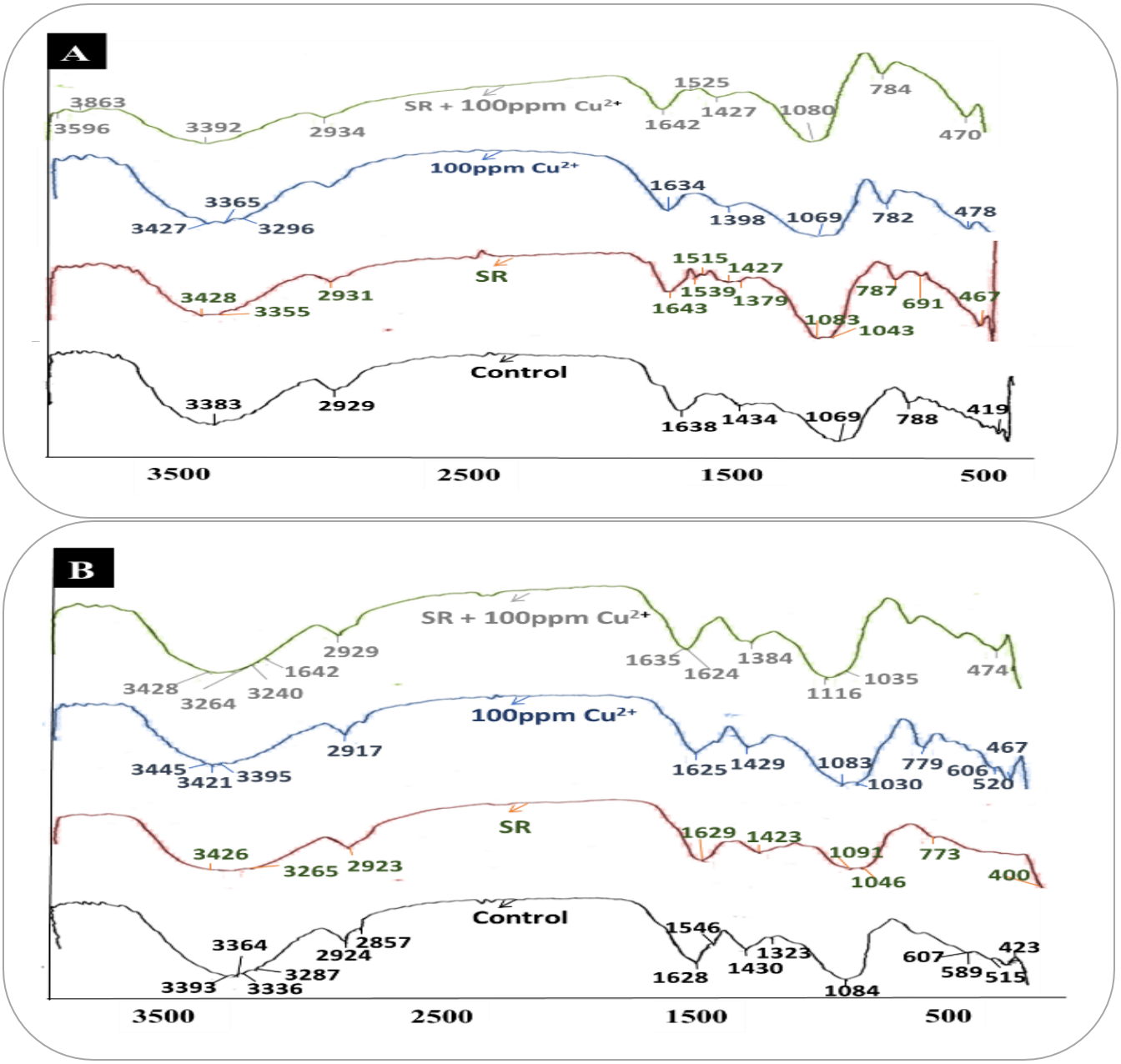

Figure 2. A & B. Comparison and characterization of Infrared spectra of root (A) and shoot (B) of *Pisum sativum*.

DISCUSSION

The present study was performed to assess the separate and combined effect of *S. rolfsii* (SR) and Cu(II) on 90-day-old plants of *P. sativum* with regard to Cu uptake and spectral features of plants after being exposed to stress/s. The Cu accumulation data depicted that green pea plant parts can uptake many times greater Cu content (T_3: 213 and T_4: 230 ppm) than recommended values of 15-50 ppm in the plant (Khurshid *et al*., 2017; Akhtar *et al*., 2016).). Soil fortification with Cu resulted in an increase in Cu accumulation by different plant parts in order of root > shoot > pods (Khurshid *et al.,* 2017). The plant accumulated more Cu in T_4 (SR + Cu) as compared to T_3 (Cu) possibly due to more mobilization of Cu during a fungal infection on the root (Akhtar *et al*., 2016; Khurshid *et al*., 2017). The BAF (capacity of the plant to uptake heavy metal from the surrounding environment) and TAF (translation from root to above-ground parts) have been used as indices for the availability/mobility of heavy metal. In the present results, values of BA and TAF were less than one which implies that green pea is not a metal bio-accumulator, where roots probably acted as the main region of metal accumulation

with its restricted transfer to the shoots (Nafisa *et al*., 2016).

FTIR is an efficient spectroscopic technique to assess the spatial differences in cell wall polymers occurring in plants due to various factor like biotic and abiotic stresses (Bhagia *et al*., 2018). FTIR absorption spectra of soil, root, and shoot in response to different treatments (T_2-T_4) depicted changes in the chemical composition of the treatments with respect to control (T_1). Peaks (3696-3600, 1633-1425, 1030, 785-497 cm^{-1}) revealed soil chemistry by indicating the presence of clay minerals such as kaolinite, illite, and calcite as well as the porous nature of the soil (Wolf, 1963; Gadsden, 1975), therefore, such soil might act as adsorbent of inorganic and organic molecules (Nayak and Singh, 2007). As compared to T_1, the peak at 3696 cm^{-1} disappeared, and peaks at 3625 and 3600 cm^{-1} shifted variably in the range of 3611-3619 cm^{-1} in the treatments T_2-T_4, which confirmed the association of Cu cations and pathogen mycelia with soil particles. A broadband intensity decreased to 3428, 3426, and 3400 cm^{-1} in T_2, T_3, and T_4, respectively might be an indication of OH stretching binding as the position and intensity of bands are affected by various exchangeable cations (Tinti *et al*., 2015). The reduction of peaks at the protein region (1620-1623 cm^{-1}) due to the effect of T_2, T_3, and T_4 relative to T_1 may specify deprotonation of C=O (amide I band). Total nitrogen content was also related to bands at 1610-1623 cm^{-1} representing amide I and II regions (Tinti *et al*., 2015). Another band at 1425 cm^{-1} in untreated soil (T_1) was due to C-H stretching and C-OH the band shifted to high wave number (1427 and1429 cm^{-1}) in T_3 and T_4, respectively may be due to higher energy on deprotonation and yielding of symmetric COO- mode. Asymmetric stretching vibration of the Si–O groups at 1030 cm^{-1}, symmetric stretch at 785 cm^{-1}, asymmetric Si–O bending mode at 695, 520, and 497 cm^{-1} was observed in T_1 but shifted to a variable extent in the soil after inoculating with the pathogen or spiking with Cu(II).

FTIR spectra of root and shoot in control (T_1) and in response to given stress/s (T_2, T_3, and T_4) showed the modification in protein, lipid, and carbohydrate regions in the range of 3426-1043 cm^{-1} (Shoaib *et al*., 2013a-c; Khurshid *et al.,* 2017; Akhtar and Shoaib, 2020). Plants grown under *S. rolfsii* stress only displayed a reduction in wave number for the N-H stretching region of the protein in the root (3383 cm^{-1}) and shoot (3399-3287 cm^{-1}) as compared to healthy plants which might be ascribed to the association of free hydrogen of primary and secondary amines with fungal mycelium. Pathogen infection also resulted in the appearance of new peaks in root (3427 and 3296 cm^{-1}) and shoot (3421 and 3445 cm^{-1}) that were due to O-H stretching vibrations assigned to water, alcohol and phenols and N-H stretching in amines (Khurshid *et al*., 2017). These regions may indicate activation of host defense mechanism against infection. The region at 3296 cm^{-1} might be due to expression of fungal protein in plant's root (Rafi *et al.,* 2017). Infection also resulted in lipid peroxidation of -CH_2/peroxides and hydroperoxides as evidenced by alteration in the intensity of bands around lipid region when compared with control (root: 2929 cm^{-1}, shoot: 2924 and 2857 cm^{-1}). The protein region in the root (1638 cm^{-1}) and shoot (1625 cm^{-1}) in control were shifted to lower peak values after pathogen inoculation that might be ascribed to amendments in the amide-I region (β-sheet and α-helix structure) due to proteolytic enzymes secreted by the pathogens. Changes in protein region showed a response to the infection. An additional peak at 1398 cm^{-1} was observed in the infected root that again indicated changes in the C-N stretch of amide-I in the protein of the host or either it could be due to protein (1369 cm^{-1}) of *S. rolfsii* (Rafi *et al*., 2017). In the healthy shoot, the peak at 1546 cm^{-1} (amide II) disappeared and 1430 cm^{-1} (cell wall polysaccharides) shifted to a low wave number due to modifications in this region after fungal infection. Changes in the structure of carbohydrates (root: 1059 cm^{-1} and shoot: 1084 cm^{-1}) were evidenced by the decrease in the intensity of bands and the formation of some new peaks that could be ascribed to the disturbance in rubisco source-sink balance and generation of photosynthate sink of green pea plant by the action of *S. rolfsii* (Akhtar and Shoaib, 2020).

In Cu-spiked soil, the changes in the intensity of bands around 3399-3287 cm^{-1} in T_3, were mainly due to free O-H and NH groups of protein when plant uptake Cu ions from the soil. Being a fundamental part of polysaccharides, the negatively charged OH ions would promote binding with positively charged Cu ions (Gnanasambandam and Protor, 2000). Shifting in bands of lipid (peroxides and hydroperoxides) spectra at wave numbers in the root (2929 cm^{-1}) and shoot (2857 and 2924 cm^{-1}) might be due to oxidative stress (lipid peroxidation). Shifting of the peaks 1628 cm^{-1} in shoot and 1638 cm^{-1} root of control suggested the involvement of the amide (I) in metal binding (Mitic-Stojanovic *et al.,* 2011). In both root and shoot, Cu also modified the amide II (1546 cm^{-1}) region. The appearance of a new peak at 1515 cm^{-1} may be linked with disruption

in the root cuticle that may cause a change in the lignin content of the root (Akhtar and Shoaib, 2020). The altered wave number of polysaccharide bands at 1059 cm^{-1} (root) and 1084 cm^{-1} (shoot) also highlighted their binding with metal ions (Shoaib *et al*., 2021).

Synergism between pathogen and Cu (T_4), resulted in peaks shifting in the homologous region as were recorded with the individual effect of *S. rolfsii* (T_2) and metal (T_3). IR spectra of both root and shoot indicated alterations in O-H (carbohydrate protein), amide I and amide II (protein), O-H bending of cell wall (polysaccharides, alcohols, and carboxylic acids), methylene (lipid) and C-O stretching cell wall (polysaccharides). In both root and shoot, many new peaks were recorded in protein and carbohydrate regions. This alternation indicated the sensitivity of protein, lipid and carbohydrate regions due to polygonal interactions of host-pathogen-metal that might be associated to the synthesis of enzymes related stress proteins of Krebs cycle, glutathione and phyto-chelatin biosynthesis (Mishra *et al*., 2006; Khurshid *et al*., 2017; Shoaib *et al*., 2021).

CONCLUSIONS

It was concluded that the root accumulated more Cu(II) restricting its movement to shoot. Soil inoculation with *S. rolfsii* increased metal uptake by the root. IR spectral analysis was found to be reliable technique to detect changes in plant cell wall dynamics as revealed by altered composition of macromolecules under separate and synergistic effect of *S. rolfsii* and Cu(II).

ACKNOWLEDGMENTS

Authors are thankful to University of the Punjab, Lahore, Pakistan for providing funds to accomplish this research work.

REFERENCES

Akhtar, S. and A. Shoaib, A. 2020. The counter defence system of antioxidants in Coelomycetous emerging human and plant pathogenic fungus *Macrophomina phaseolina* against copper toxicity. Environmental Science and Pollution Research, 27: 597-606.

Akhtar, S., A. Shoaib, N. Akhtar and R. Mehmood. 2016. Separate and combined effects of *Macrophomina phaseolina* and copper on growth, physiology and antioxidative enzymes in *Vigna mungo* L. Journal of Animal and Plant Sciences, 26: 1339-1345.

Alloway, B. J. 2013. Sources of heavy metals and metalloids in soils. *In:* Heavy Metals in Soils Environmental Pollution, ed. B. J. Alloway (Dordrecht: Springer Netherlands).

Bağcıoğlu, M., A. Kohler, S. Seifert, J. Kneipp and B. Zimmermann. 2017. Monitoring of plant–environment interactions by high-throughput FTIR spectroscopy of pollen. Methods in Ecology and Evolution, 8: 870-80.

Bhagia, S., X. Meng, B.R. Evans, J.R. Dunlap, G. Bali, J. Chen, K.S. Reeves, H.C. Ho, B.H. Davison, Y. Pu and A.J. Ragauskas. 2018. Ultrastructure and enzymatic hydrolysis of deuterated Switchgrass. Scitific Report, 8: 13226.

Gadsden, J. A. 1975. Infrared spectra of minerals and related inorganic compounds. London: Butterworth & Co. (Publishers) Ltd. pp. 277.

Gnanasambandam, R. and A. Protor. 2000. Determination of pectin degree of esterification by diffuse reflectance Fourier transform infrared spectroscopy. Food Chemistry, 68: 327-332.

Khurshid, S., A. Shoaib, A. Javaid, F. Akhtar, M. Shafiq and U. Qaisar. 2017. Management of Fusarium wilt of tomato by soil amendment with *Cenchrus pennisetiformis* under chromium stress. Physiology and Molecular Plant Pathology, 97: 58-68.

Lahlali, R., Y.F. Jiang, S. Kumar, C. Karunakaran, X. Liu, F. Borondics, E. Hallin and R. Bueckert. 2014. ATR-FTIR spectroscopy reveals involvement of lipids and proteins of intact pea pollen grains to heat stress tolerance. Frontier in Plant Sciences, 5: 747-753.

Largo-Gosens, A., M. Hernández-Altamirano, L. García-Calvo, A. Alonso-Simón, Álvarez and J.L. Acebes. 2014. Fourier transform mid-infrared spectroscopy applications for monitoring the structural plasticity of plant cell walls. Frintier in Plant Sciences, 5: 303-309.

Mazurek, S., A. Mucciolo, B.M. Humbel and C. Nawrath. 2013. Transmission Fourier transform infrared microspectroscopy allows simultaneous assessment of cutin and cell-wall polysaccharides of Arabidopsis petals. Plant Journal, 74: 880-891.

Mishra, S., S. Srivastava, R.D. Tripathi, R. Govindarajan, S. V. Kuriakose and M.N.V. Prasad. 2006. Phytochelatin synthesis and response of antioxidants during cadmium stress in *Bacopa monnieri* L. Plant Physiology and Biochemistry, 44: 25-37.

Mitic-Stojanovic, D.L., A. Zarubica, M. Purenovic, D. Bojic, T. Andjelkovic and A. L. Bojic. 2011. Biosorptive

removal of Pb^{2+}, Cd^{2+} and Zn^{2+} ions from water by *Lagenaria vulgaris* shell. Water SA, 37: 303-312.

Nafisa, A. Shoaib and A. Javaid. 2013. Growth of *Pisum sativum* under single or combined action of *Sclerotium rolfsii* and copper [Cu(II)]. International Journal of Agriculture and Biology, 15: 1363-1366.

Nafisa, A. Shoaib, M. Shafiq and A. Javaid. 2016. Effect of *Sclerotium rolfsii* on uptake of heavy metal copper in pea (*Pisum sativum*). International Journal of Agriculture and Biology, 18: 1363-1366.

Nayak, P.S. and B.K. Singh. 2007. Instrumental characterization of clay by XRF, XRD and FTIR. The Bulletin of Materials Science, 33: 235-238.

Nikalje, G.C., J. Kumar, T. D. Nikam and P. Suprasanna, 2019. FT-IR profiling reveals differential response of roots and leaves to salt stress in a halophyte *Sesuvium portulacastrum* (L.). Biotechnology Reports, 23: Article ID e00352.

Printz, B., S. Lutts, J. F. Hausman and K. Sergeant. 2016. Copper trafficking in plants and its implication on cell wall dynamics. Frontier in Plant Sciences, 6: 601-609.

Rafi, S., A. Shoaib, Z. A. Awan, N. B. Rizvi and M. Shafiq. 2017. Chromium tolerance, oxidative stress response, morphological characteristics, and FTIR studies of phytopathogenic fungus *Sclerotium rolfsii*. Folia Microbiologica, 62: 207-219.

Sana, N., A. Javaid and A. Shoaib, A. 2017. Effect of NPK fertilizers and commercial biofertilizers on southern blight disease and plant growth in chili. Bangladesh Journal of Botany, 46: 659-666.

Sana, N., A. Shoaib, A. Javaid and A. K. Khan. 2016. Phytochemical management of collar rot of chili with leaf biomass of *Eucalyptus camaldulensis*. Pakistan Journal of Phytopathology, 28**:** 19-24.

Shoaib, A., M. Akhtar, A. Javaid, A. Haider, Z. Nisar and S. Javed. 2021. Antifungal potential of zinc against leaf spot disease in chili pepper caused by *Alternaria alternata*. Physiology and Molecular Biology of the Plants, 27: 1361-1376.

Shoaib, A., S. Abbas, Z. Nisar, A. Javaid and S. Javed 2022. Zinc highly potentiates the plant defense responses against *Macrophomina phaseolina* in mungbean. *Acta Physiologiae Plantarum*, 44: 1-17.

Shoaib, A., N. Akhtar, Nafisa and A. Aftab, 2013c. Fourier Transform-Infrared Spectroscopy to monitor modifications in canola biochemistry caused by *Alternaria destruens*. Pakistan Journal of Phytopathology, 25: 105-109.

Shoaib, A., N. Aslam and N. Aslam. 2013b. *Trichoderma harzianum*: Adsorption, desorption, isotherm and FTIR studies. Journal of Animal and Plant Sciences, 23: 1460-1465.

Shoaib, A., N. Aslam, M. M. Athar, S. Akhtar, Nafisa and S. Khurshid. 2013a. Removal of Cr(VI) ions through bread mold fungus. Polish Journal of Environmental Studies, 2: 171-176.

Thumanu, K., M. Sompong, P. Phansak, K. Nontapot and N. Buensanteai. 2015. Use of infrared microspectroscopy to determine leaf biochemical composition of cassava in response to *Bacillus subtilis* CaSUT007. Journal of Plant Interactions,10: 270-9.

Tinti, A., V. Tugnoli, S. Bonora and O. Francioso. 2015. Recent applications of vibrational mid-Infrared (IR) spectroscopy for studying soil components: a review. Journal of Central European Agriculture, 16: 1-22.

Wilson, R.H., A.C. Smith, M. Kačuráková, P.K. Saunders, N. Wellner and K.W. Waldron. 2000. The mechanical properties and molecular dynamics of plant cell wall polysaccharides studied by Fourier-transform infrared spectroscopy. Plant Physiology, 124: 397-405.

Wolf, R. G. 1963. Structural aspects of kaolinite using infrared absorption. American Mineralogist, 48: 390.

Yashim, Z.I., I. O. Kehinde and M. Hannatu. 2014. A study of the uptake of heavy metals by plants near metal-scrap dumpsite in Zaria, Nigeria. Journal of Applied Chemistry, 4: 1-5.

Contribution of Authors:

Amna Shoaib	:	Designed experiment and wrote the manuscript
Nafisa	:	Performed experiments and edited the manuscript
Ghanwa Riaz	:	Edited the manuscript
Qudsia Fatima	:	Analysis and interpretation of data
Uswa Fatima	:	Analysis and interpretation of data